JOURNAL OF GEOPHYSICAL RESEARCH, VOL. 97, NO. D17, PAGES 18,533–18,546, NOVEMBER 30, 1992

Budget Analysis of the Boundary Layer Grid Flights During FIFE 1987

A. K. BETTS

Atmospheric Research, Middlebury, Vermont

R. L. DESJARDINS

Land Resource Research Centre, Agriculture Canada, Ottawa, Ontario

J. I. MACPHERSON

Institute for Aerospace Research, Ottawa, Ontario, Canada

An aircraft grid pattern was flown by the Canadian Twin Otter to map the low-level fluxes and structure over the First International Satellite Land Surface Climatology Project (ISLSCP) Field Experiment (FIFE) research area in 1987. The time dependence and horizontal advection of heat and moisture were extracted from these flights, combined with surface flux measurements and boundary layer top measurements from radiosondes, to analyze the boundary layer budget using a mixed layer model. The results confirm the suggestion of an earlier study that the boundary layer top entrainment (when parameterized using the buoyancy flux) is nearly double the value used by many modeling studies. Both surface and aircraft data have been revised, and it now appears that the direct measurements of the sensible and latent heat fluxes by the aircraft underestimated these fluxes by about 20%, because of filtering and undersampling of long wavelength contributions.

1. INTRODUCTION

The First International Satellite Land Surface Climatology Project (ISLSCP) Field Experiment (FIFE) included an extensive program of surface and atmospheric boundary layer (ABL) measurements. Boundary layer aircraft flights were designed to study the heat and moisture fluxes and budgets over the FIFE site for comparison with surface measurements of sensible and latent heat flux. *Betts* [this issue] discusses the budget methods used to analyze the FIFE ABL flights. *Betts et al.* [1990] used pairs of aircraft stacks, flown upwind and downwind of the FIFE surface network under nearly clear skies, to evaluate a volumetric budget using a mixed layer model. They found that budget estimates of the surface sensible and latent heat flux agreed well with the surface flux measurements but that the direct aircraft measurements underestimated the low-level fluxes. Their analysis also suggested that using data from a single aircraft, the time derivative and the horizontal spatial derivatives could be separated sufficiently to perform useful budget analyses for the ABL. In addition, they found higher than expected ABL top entrainment.

This paper continues the budget analysis using a second aircraft flight pattern, in which a "grid" (Figure 1) of east-west legs was flown at low levels (75–100 m) to map the near-surface fluxes over the FIFE area. We compare the aircraft measurements with the surface flux data, the surface meteorological data from the portable automated meteorological (PAM) stations, and the radiosonde data; we also assess the usefulness of this grid pattern for the budget analysis of the ABL. These FIFE grid flights again indicate the importance of both the fluxes at the ABL top inversion and the horizontal advection in the ABL thermodynamic budget. They also confirm the conclusion of *Betts et al.* [1990] that the direct aircraft measurements of the sensible and latent heat fluxes underestimated the surface fluxes. However, the underestimate has been reduced since *Betts et al.* [1990]. The flux data for the surface "Bowen ratio" sites have been revised downward, following recalibration of their surface radiometers. Three sources for the residual underestimation by the aircraft have subsequently been identified. The first, now corrected for the October 1987 flights, lay in the choice of the processing algorithm for the vertical eddy wind components. Reprocessing the aircraft flux data using the vertical wind from the Litton inertial navigation system, rather than the aircraft Doppler winds for low-frequency filtering [*MacPherson*, 1990], gave on average 13% higher fluxes and a higher covariance. The Litton inertial navigation method of processing has been chosen for the subsequent 1989 FIFE flights. The high-pass filtering of the data (see section 2) accounts for about 17% of the flux underestimate, and the limited length of the 15-km runs is responsible for the residual flux underestimate of 4%, because longer wavelengths are not sampled. These new budget analyses also confirm that the entrainment at the top of the ABL in FIFE is nearly double that suggested by the simplest dry mixed layer models.

Paper number 91JD03173.
0148-0227/92/91JD-03173$05.00

2. INSTRUMENTATION

The Canadian National Aeronautical Establishment (NAE) Twin Otter atmospheric research aircraft was instrumented to measure three orthogonal components of atmospheric motion: air temperature, CO_2, and water vapor fluctuations [*MacPherson et al.*, 1985]. It was also instrumented with a slow response Cambridge dew point system for humidity measurements. All signals are sampled at 16 Hz, low-pass filtered at 5 Hz, and high-pass filtered at 0.012

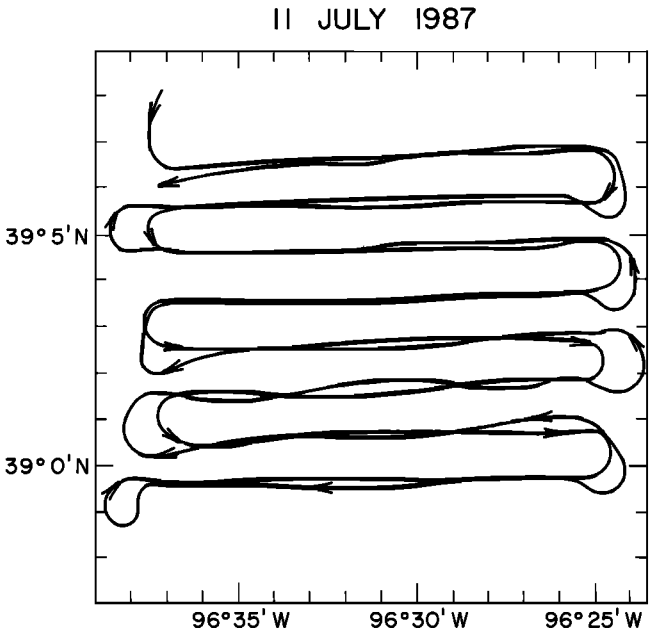

Fig. 1. Grid pattern flown by Canadian National Aeronautical Establishment (NAE) Twin Otter on July 11, 1987.

Hz. This sampling corresponds to spatial scales ranging from about 11 m to 4.6 km at the usual aircraft speed of 55 m s^{-1}. The data recording and processing followed the procedures discussed by *Desjardins et al.*, [1986, 1989]. The 0.012-Hz high-pass filter was used to minimize the variability from run to run. It produces an underestimate of the turbulent fluxes [*Desjardins et al.*, this issue], which for these flights is about 17%, but it is useful when searching for other physical sources of variability.

3. METHODOLOGY

3.1. *Flight Plan*

A typical flight plan (for July 11, 1987) is shown in Figure 1. The Twin Otter flew sixteen 15-km runs (over the FIFE site) in an east-west direction, following the grid pattern shown. The north-south spacing between runs is 1.85 km. The pattern was flown from north to south (eight runs) and then repeated from south to north in the reverse direction. This gives the same average time for each pair of runs on the same track, with reverse headings for each pair. The actual altitude above the rolling terrain varied slightly but averaged about 100 m. The runs shown in Figure 1 were made between 1555 and 1728 UTC, during reasonably clear conditions with strong winds from the south-southwest. The use of a single aircraft with one set of sensors simplifies the measurement of horizontal gradients, provided the sensors do not drift with time. It is difficult, however, to accurately separate spatial derivatives from time derivatives in the rapidly time-dependent situation characteristic of the daytime ABL over land. The budget analyses presented here depend on one crucial assumption: we assume a linear trend with time and constant advection for roughly 90 min. There are a few cases where this is clearly not satisfied, and these are discussed later.

TABLE 1. Summary Data for Grid Flights

Flight	Date, 1987	Time, UTC	Mean Wind, deg/m s^{-1}	Inversion Height, m
July 11	11	1555–1728	192/13.3	830 ± 100
Aug. 15	23	1603–1741	192/8.6	740 ± 160
Aug. 15	24	2007–2146	188/11.6	800 ± 50
Oct. 7	34	1646–1826	344/6.7	780 ± 40
Oct. 7	35	2008–2147	350/4.5	1575 ± 50
Oct. 11	37	1714–1905	243/1.4	1000 ± 100
Oct. 12	39	1714–1900	291/1.5	540 ± 100
Oct. 13	40	1355–1556	195/10.1	230 ± 80

3.2. *Summary of Flights*

Table 1 summarizes the flights analyzed in this paper, together with the mean wind and inversion height. Time is given as coordinated universal time (UTC); central daylight time is UTC minus 5 hours. Wind conditions range from light winds of 1–2 m s^{-1} (October 11 and 12) to strong winds of 13 m s^{-1} on July 11. There is a considerable range of mixed layer depths (estimated from radiosondes). Most are late morning or afternoon flights. However, the last flight on October 13 started near sunrise, when the mixed layer was very shallow (≤100 m), comparable to the level of the aircraft measurements. During this flight the ABL depth grew to ≈350 m, and the aircraft and surface measurements also showed the effect of a sudden change in the ABL top entrainment; therefore only part of this flight was used for the budget analysis. Three flights were conducted in July and August, when the surface vegetation was actively growing and the surface Bowen ratio for these flights is low; five were in October after the vegetation had mostly died, and the surface Bowen ratio for these flights is high.

3.3. *Budget Method*

The derivation of the budget equations and the use of the mixed layer model are discussed in detail by *Betts* [this issue]. In this paper we used mixed layer budgets for mean potential temperature (θ) and mean mixing ratio (q):

$$\partial\theta/\partial t + u\partial\theta/\partial x + v\partial\theta/dy = (F_{s\theta} - F_{i\theta})/\rho C_p Z_i \qquad (1a)$$

$$\partial q/\partial t + u\partial q/\partial x + v\partial q/dy = (F_{sq} - F_{iq})/\rho L Z_i \qquad (1b)$$

where F_θ and F_q are the fluxes of sensible and latent heat (in watts per square meter), and the subscripts s and i indicate the surface and the inversion base, respectively. Leg averages at the aircraft flight level were taken as representative of the mixed layer means. The analysis of *Betts et al.* [1990] supports this assumption. The mean advection along the flight legs, $u\partial\theta/\partial x$, $u\partial q/\partial x$, was found by separately averaging u for all the legs, and also $\partial\theta/\partial x$ and $\partial q/\partial x$, using the mean trend line for each leg for the gradients. Because the legs are flown in pairs in both directions, the time derivative approximately cancels in the pattern average. We then separated the time and north-south (y) derivatives by using linear regression on the means for the 16 legs. This assumes constant gradients in time and space during the pattern, a restrictive assumption that may not always be satisfied. One particular example is the late-afternoon flights, when $\partial^2\theta/\partial t^2$ is typically negative. When linear regression is applied to a pattern flown from north to south and then back, it converts a quadratic θ dependence into its linear component

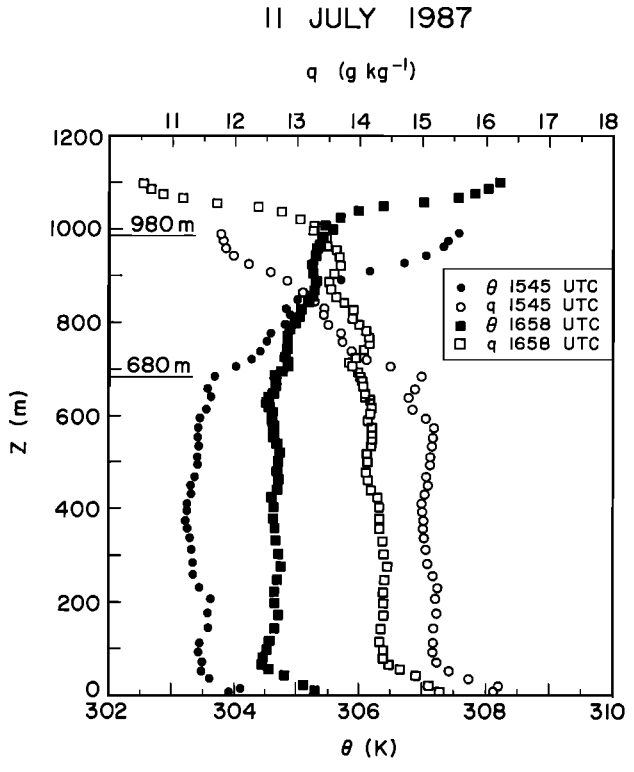

Fig. 2. Radiosonde soundings on July 11, 1987, showing top of mixed layer.

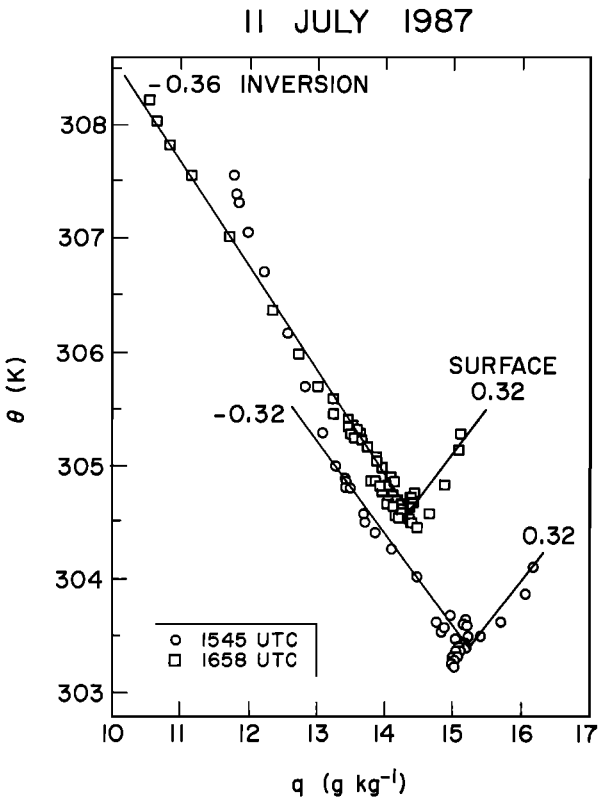

Fig. 3. The (θ,q) plot of July 11 soundings showing the mixing lines which give the inversion level Bowen ratio. The surface Bowen ratio of 0.32 is based on surface flux measurements.

in time and gives a spurious spatial gradient $\partial\theta/\partial y$. Unfortunately, with a single aircraft there is no other simple way of separating time and space derivatives. We use the surface and sounding data to identify cases where the linearity assumption appears not to be satisfied (see later discussion).

3.4. *Estimation of Budget Terms*

Each of the terms in (1*a*) and (1*b*) was estimated separately, together with an estimate of the error. The terms were then summed to give a residual and the errors combined (as random errors) to give an error estimate for the residual (see Tables 4 and 5).

The vertical flux gradient involves three separate components: the surface fluxes, the inversion fluxes, and the ABL depth. The 1987 FIFE had a network of 18–20 surface stations measuring surface parameters and the surface heat and moisture fluxes. A subset of 14 surface flux sites were selected as representative of the FIFE area. To estimate the overall mean surface fluxes over the FIFE area, we averaged the 30-min mean values from these 14 surface flux sites, then interpolated and averaged these area means for the time period of each aircraft flight. We estimated the accuracy of the mean surface flux values by dividing the variance between sites by $(N-1)^{1/2}$, where N is the number of sites.

The ABL depth was chosen as the base height of the inversion (Z_i), determined from the radiosonde ascents. There were typically two to three ascents at about hourly intervals near the time of each flight, so we averaged these values and estimated an error from the variability. Figure 2 shows the two soundings close to the pattern time on July 11. The inversion bases marked as 680 and 980 m in Figure 2 are the approximate heights where θ sharply increases and q sharply decreases. For the 1658 UTC sounding there is a weakly stable layer from 630 to 980 m above a nearly constant potential temperature layer (see also Figure 3), so there is some ambiguity in the definition of the "mixed" layer. Thus this method of finding Z_i is not accurate, and it is an appreciable source of error in our analysis. Single vertical profiles through the ABL take only 5–10 min, and they do not average over the considerable spatial variability. Typically, the ABL is growing with time, but it would not be correct to assume linearity between the two profiles in Figure 2. Fluctuations of ABL depth can occur which are associated with mesoscale eddy structure or with the advection of different air masses over the network. Estimates of inversion base height are also available for two analysis days (July 11 and August 15) from a single vertically pointing sodar. For July 11 these give an average inversion base height of 800 m during the aircraft pattern, in agreement with the two soundings. Maps of the inversion base by lidar will also give a better mean, if these become available for any of our analysis days.

The inversion level fluxes were not measured during these grid flights in FIFE 1987. The mixed layer model discussed by *Betts* [this issue] was therefore used to estimate equivalent mixed layer top fluxes, using a specified entrainment parameter, A_R (see section 3.5), and the Bowen ratio at the inversion β_i. These equivalent mixed layer top fluxes include both the effects of boundary layer growth and subsidence on the evolution of the mean ABL properties. β_i was also estimated from the radiosonde ascents by plotting (θ,q) mixing diagrams [*Betts*, 1985; *Betts et al.*, 1990], which show the coupling of the θ and q gradients through the inversion

TABLE 2. Fluxes of Sensible and Latent Heat at the Surface and Calculated at the Inversion

		Surface Measurements			Inversion Level		
Date, 1987	Flight	$F_{s\theta}$, W m^{-2}	F_{sq}, W m^{-2}	Bowen Ratio, β_s	$F_{i\theta}$, W m^{-2}	F_{iq}, W m^{-2}	Bowen Ratio, β_i
July 11	11	120 ± 14	372 ± 14	0.32 ± 0.04	−71 ± 31	213 ± 94	−0.34 ± 0.02
Aug. 15	23	118 ± 12	346 ± 17	0.34 ± 0.04	−64 ± 28	137 ± 79	−0.47 ± 0.18
Aug. 15	24	79 ± 10	351 ± 16	0.23 ± 0.03	−59 ± 26	270 ± 121	−0.22 ± 0.02
Oct. 7	34	307 ± 19	68 ± 5	4.51 ± 0.43	−127 ± 54	115 ± 72	−1.10 ± 0.50
Oct. 7	35	205 ± 14	60 ± 6	3.42 ± 0.41	−93 ± 40	186 ± 80	−0.50 ± 0.01
Oct. 11	37	318 ± 19	56 ± 7	5.68 ± 0.79	−122 ± 52	1 ± 1	−100.00 ± 10
Oct. 12	39	282 ± 18	59 ± 6	4.78 ± 0.57	−126 ± 54	238 ± 105	−0.53 ± 0.06
Oct. 13	40	139 ± 10	41 ± 5	3.39 ± 0.48	−56 ± 24	23 ± 14	−2.40 ± 1.00

Here F_θ indicates sensible heat and F_q indicates latent heat; subscripts s and i refer to surface and inversion levels, respectively. Fluxes at the inversion were calculated using the entrainment parameter, $A_R = 0.38$.

where the entrainment is taking place. Figure 3 shows an example for the two soundings on July 11. We found a value

$$\beta_i = (C_p/L)(\partial\theta/\partial q)_i \tag{2}$$

through the ABL top inversion for each ascent, averaged these values to give a mean for each flight, and roughly estimated the error from the variability between soundings. In Figure 3 we only have two values for July 11: $\beta_i = -0.32$ and -0.36. Aircraft legs in the inversion would give a better mean estimate of β_i, but these were not available. In some cases there were sudden changes between soundings associated with the disappearance, for example, of a dry layer, as it was completely entrained into the ABL. In discussing the individual days, we note cases where this change could be seen in the surface and aircraft data. Figure 3 also shows the slope corresponding to the mean surface Bowen ratio, $\beta_s = 0.32$, computed from the surface flux measurements during the aircraft pattern. It shows that the gradient off the surface determined by the radiosonde is roughly consistent with this β_s, although the sonde data are neither sufficiently accurate nor representative enough to adequately determine the surface Bowen ratio from single soundings. *Sugita and Brutsaert* [1990], in a larger study of the FIFE data, found similar agreement between the mean surface Bowen ratio and the low-level $(C_p/L)\partial\theta/\partial q$ gradient from soundings.

3.5. *Model for Inversion Level Fluxes*

Since we had no inversion level data and had aircraft data at only one level, we made the mixed layer assumption for the ABL and used a mixed layer model closure to estimate inversion level fluxes. The analysis is given by *Betts* [this issue], based on the earlier work of several authors, who determined an inversion level buoyancy flux from a surface buoyancy flux using a closure parameter A_R

$$F_{i\theta v} = -A_R F_{s\theta v} \tag{3}$$

From (3) we can extract the inversion level fluxes of sensible heat θ and latent heat q [*Betts*, this issue]:

$$F_{i\theta} = -A_R F_{s\theta}(1 + \delta\varepsilon/\beta_s)/(1 + \delta\varepsilon/\beta_i) \tag{4a}$$

$$F_{iq} = F_{i\theta}/\beta_i \tag{4b}$$

The subscripts s and i denote surface and inversion level fluxes, respectively. β_s and β_i are the surface and inversion level Bowen ratios; β_s is found from the average of the 14 surface flux stations, and β_i from applying (2) to the soundings through the inversion. We took the thermodynamic parameter $\delta\varepsilon = 0.608 C_p T/L = 0.07$ as constant, since the uncertainties in β_s and β_i are much larger than variability of $\delta\varepsilon$.

The parameter A_R was introduced as a simple closure for the buoyant energy available for entrainment of inversion level air [*Betts*, 1973; *Carson*, 1973; *Tennekes*, 1973; *Stull*, 1976]. Since both inversion level fluxes are proportional to A_R, it is a crucial parameter in our analysis. The authors, cited previously, suggested $A_R \approx 0.2$, and this has generally been regarded as a satisfactory value for dry convective layers, in the absence of shear. However, *Betts et al.* [1990] found, from a set of six FIFE 1987 flights in high-wind regimes, a significantly larger estimate of $A_R = 0.43$ (± 0.12). Here we are analyzing a different set of eight flights for FIFE 1987 (only half with strong winds), but again we find (see section 4) that a large value of $A_R = 0.38$ (± 0.16) gives sensible and latent heat fluxes at the inversion that best satisfy the budget equations. It is possible that turbulence generated by shear is contributing significantly to the entrainment; however, even the low-wind cases had values of $A_R \approx 0.4$ (see below).

Table 2 gives the inversion level fluxes calculated from (4) for $A_R = 0.38 \pm 0.16$, together with the measured surface fluxes and the corresponding Bowen ratios. We use watts per square meter throughout as units for the fluxes. Estimates of the errors in each term are also given. From these fluxes we computed the vertical flux gradients in (1), together with an error estimate found by combining the errors of the separate inputs, assuming all errors to be random. Note that these vertical flux gradients depend significantly on A_R.

3.6. *Error Analysis*

The error analysis is not sophisticated, as can be seen from our methods of assessing the errors of individual measurements. Some important terms such as ABL depth, Z_i, and β_i are not well known, because we have only two or three point values of unknown areal representativity. Others, such as the time and y derivatives, have been found by linear regression. This gives an error estimate, but the method assumes constant gradients during a flight, which in some cases is questionable (see section 4). There is quite a wide spread in the surface flux measurements, each of which

TABLE 3. Estimates of Entrainment Parameter Using Advection Term and With Advection Terms Set to Zero

Date, 1987	Flight	A_R (adv)	Normalized Residual (adv)	A_R (zero)	Normalized Residual (zero)	V_A, m s^{-1}	V_S, m s^{-1}	$\overline{u'w'}$ cm^2 s^{-2}	A_{Ru}*
Jul. 11	11	0.53	1.40	(0.30)	0.22	13.6	9.6	0.71 ± 0.10	0.60 ± 0.05
Aug. 15	23	0.49	−0.58	(0.15)	1.46	8.6	5.9	0.34 ± 0.07	0.36 ± 0.04
Aug. 15	24	(0.07)	−1.30	0.06	−0.24	11.6	7.5	0.48 ± 0.11	0.51 ± 0.07
Oct. 7	34	(0.65)	−0.10	0.29	−0.39	6.7	4.0	0.31 ± 0.10	0.27 ± 0.03
Oct. 7	35	(0.57)	1.28	0.27	−0.04	4.5	3.5	0.21 ± 0.14	0.23 ± 0.03
Oct. 11	37	0.51	−0.14	(0.41)	0.36	1.4	1.4	0.00	0.20 ± 0.0
Oct. 12	39	0.42	−0.04	(0.35)	−0.53	1.5	1.2	0.00	0.20 ± 0.0
Oct. 13	40	0.49	1.25	(0.30)	0.16	10.1	7.0	0.52 ± 0.13	0.92 ± 0.16
Mean		0.47 ± 0.17		0.27 ± 0.11					

A_R is entrainment parameter estimated from budgets. A_{Ru}* is calculated using the shear stress $u'w'$. Values in parentheses were rejected.

perhaps represents different individual sites. A more refined analysis may give better estimates of the surface areal mean flux, but it will not affect our analysis much. Despite its weaknesses this simple error analysis is very useful in assessing which terms are poorly known in a given budget. We combined the error estimates in individual terms to give an overall error estimate and then used this to normalize the residuals in each budget.

4. BUDGET RESULTS

As is usually the case with meteorological data, every day and every flight had unique characteristics. Our analysis involves an interplay between an idealized model and data for individual days; data which do not always satisfy the assumptions of the model. As a result, for some days, choices had to be made based on supporting evidence. We first present an overview of our budget results and then discuss the individual days in detail, together with the basis of any subjective decisions that were made in analysis.

4.1. *Determination of Closure Parameter A_R*

Since we have no measurements of inversion level fluxes (only the inversion level Bowen ratio), these have been determined using (2) and (4). Thus our budget results depend on knowing the closure parameter A_R. We varied A_R and examined the residuals (normalized by the error estimate) for the heat and water budgets for each flight. Because the inversion level Bowen ratios are negative, increasing A_R reduces the θ budget residual but increases the q budget residual. For each flight we found the value of A_R for which the normalized θ and q budget residuals were equal. This represents an optimum fit to the heat and moisture budgets, because it is, to close approximation, an average of the two values of A_R that would give zero residuals for the separate heat and moisture budgets. Table 3 shows these values of A_R and the normalized residual calculated from the full budget. These normalized residuals are marked (adv), indicating that advection terms are included. The time derivatives and surface fluxes are known quite accurately in the budgets. The advection terms not only have generally larger errors, however, but their estimation also depends critically on the assumption of linear trends in time and space (north-south). There are several budgets where this linearity assumption appears invalid on the basis of supporting measurements (see section 5), so we also reduced the advection terms to zero and computed a second optimum value of A_R and a corresponding normalized residual for each budget. Table 3 shows these in the columns marked (zero).

A normalized residual ≈1 in Table 3 means a residual comparable to the error estimate. We see quite a range of values of A_R; we also note that the budgets are sensitive to the horizontal advection terms. Removing the advection terms in all cases reduces the "best fit" value of A_R, although in some cases the fit is worse. Including the advection terms gives a mean $A_R = 0.47 \pm 0.17$ and dropping them gives 0.27 ± 0.11, so it is clear that they play a crucial role in the budget and in our determination of the entrainment closure parameter A_R.

Many budgets have significant cold or moist advection (see Tables 4 and 5 later), so that dropping the advection terms reduces the entrainment of warm dry air needed to balance the budget. We reviewed the advection terms closely, and for flights 24, 34, and 35 we found convincing evidence (see section 5) that the critical assumption of linear trends in time was not satisfied. This introduced a significant error in the north-south advection derived from linear regression. For these three flights we chose the solutions with both advection terms reduced to zero, rather than introduce clearly spurious terms into the budget. Since we do not in fact know that there was no horizontal advection, we retained the error estimates on the horizontal advection. Of the remaining five flights the first (flight 11) is clearly improved if we were to reject the advection, but we have no evidence to justify this. On the other hand, the second (flight 23) is much improved by the advection terms. For the two low-wind days (flights 37 and 39) the advection terms look good and improve the budget a little, although they are small. For the last flight (flight 40) the advection estimate looks good (a repeated pattern was flown; see section 5.5). The budget errors are probably from other causes, as this was a flight just after sunrise when the ABL was growing rapidly. Selecting the eight A_R values not in parentheses (three with the advection terms zeroed) gives a value for the entrainment closure parameter of $A_R = 0.38 \pm 0.16$. We used this mean value for the subsequent analysis and the variance as an error estimate on A_R. As discussed previously, many authors have suggested $A_R \approx 0.2$ for buoyantly driven entrainment into dry mixed layers. Despite considerable scatter our mean value of 0.38 ± 0.16 is nearly double the value widely used in mixed layer modeling. *Betts et al.* [1990], from another set of six FIFE flights, found a similar value of 0.43 ± 0.12. (The subsequent corrections to the

TABLE 4. Sensible Heat Budgets

Date, 1987	Flight	$\partial\theta/\partial t$, W m^{-3}	$u\partial\theta/\partial x$, W m^{-3}	$v\partial\theta/\partial y$, W m^{-3}	$\partial F_\theta/\partial z$, W m^{-3}	Residual, W m^{-3}	Normalized (adv)	Residual (zero)
July 11	11	0.224 ± 0.004	−0.010 ± 0.013	0.131 ± 0.019	0.231 ± 0.050	0.114 ± 0.055	2.07	(−0.11)
Aug. 15	23	0.286 ± 0.005	−0.020 ± 0.018	−0.038 ± 0.018	0.247 ± 0.067	−0.019 ± 0.072	−0.27	(0.54)
Aug. 15	24	0.100 ± 0.004	0.004 ± 0.003	−0.044 ± 0.018	0.173 ± 0.037	−0.113 ± 0.041	(−2.73)	−1.76
Oct. 7	34	0.484 ± 0.006	−0.041 ± 0.019	0.219 ± 0.014	0.556 ± 0.079	0.106 ± 0.086	(1.23)	−0.83
Oct. 7	35	0.171 ± 0.007	−0.014 ± 0.006	0.103 ± 0.13	0.189 ± 0.027	0.072 ± 0.032	(2.25)	−0.56
Oct. 11	37	0.478 ± 0.010	0.011 ± 0.012	−0.018 ± 0.003	0.440 ± 0.071	0.031 ± 0.073	0.42	(0.52)
Oct. 12	39	0.641 ± 0.021	0.101 ± 0.036	0.030 ± 0.005	0.756 ± 0.175	0.017 ± 0.180	0.09	(−0.64)
Oct. 13	40	0.843 ± 0.014	−0.062 ± 0.078	0.574 ± 0.051	0.846 ± 0.315	0.508 ± 0.329	1.55	(−0.01)

Columns 3–7 are all converted to units of watts per cubic meter (W m^{-3}).

surface flux data do not significantly affect this number.) Table 3 also lists the mean wind speed at the aircraft flight level (V_A) and at the surface mesonet stations (V_S) for each individual flight. Shear-generated or wave-generated turbulence could be driving additional entrainment, but the widely scattered values of A_R are not well correlated with wind speed. *Stull* [1988, p. 483] gives formulae for estimating entrainment parameters, when both the surface stress and the heat flux are important in driving entrainment. His formulae (in our notation) give A_R as the root of the equation:

$$A_R^2 - 2(1 + A_R)[C_1 + C_2\theta_v u_*^3/gF_{s\theta v}Z_i] = 0 \qquad (5)$$

where $C_1 = 0.0167$, $C_2 = 0.5$, and u_* is the surface friction velocity. This formula gives $A_R = 0.2$ for $u_* = 0$. *Brutsaert and Sugita* [1990] give values of $u_* \approx 1$ m s^{-1} for the high-wind days of July 11, August 15, and October 13 in our data set. If we substitute this estimate of u_*, together with values for $F_{s\theta v}$, and Z_i in (5) the shear generation term completely dominates and (5) gives $A_R \approx 1$; this value is even higher than the value we have found. Although it seems likely that shear production of turbulence is important, this estimate of A_R is much too large. Thus either the estimates of u_* given by *Brutsaert and Sugita* [1990] are too high (by perhaps 30%) or the coefficient C_2 in (5) is much smaller than 0.5. The aircraft measurements of $u_*^2 = \overline{u'w'}$ for each flight are given in Table 3 along with the corresponding solution for A_R from (5), shown as A_{Ru_*}. The error estimate is based solely on the error estimate in u_*^2; we do not know the errors in the coefficients C_1 and C_2 in (5). The aircraft stress measurements are at 70–100 m above the surface and are smaller than those of *Brutsaert and Sugita* [1990]. As a result they give values of A_{Ru*} that are more consistent with our budget analysis. (However, the aircraft stress measurements may also be underestimates like the heat and moisture fluxes.) The two largest values of A_{Ru_*} are for July 11, when winds were strong, and October 13, when winds were strong and the boundary layer was shallow. However, for the two light-wind days the stress term in (5) is insignificant and (5) gives $A_{Ru_*} = 0.2$, whereas our budget analyses (which look good for these flights) give significantly higher values of $A_R \approx 0.4$. Clearly, more studies and a deeper understanding of ABL top entrainment are needed to predict daytime ABL evolution. We present budget tables and the subsequent analysis using a single mean value of A_R in section 4.2.

4.2. *Heat and Moisture Budgets*

Tables 4 and 5 summarize the budgets for the eight flights using our mean value of $A_R = 0.38 \pm 0.16$. The last two columns on the right-hand side of these tables show the residuals normalized by the error estimate: one uses the advection terms, the second has zero horizontal advection. These differ from those in Table 3, because we have used one single value of A_R, rather than a best fit value for each flight. As a whole these budgets are encouraging. The values not in parentheses are the ones we have accepted, but we include the rejected ones (in parentheses) to show the importance of the horizontal advection. The normalized moisture residuals are satisfactorily all ≤ 1. Three heat budget residuals are ≥ 1. We have no explanation for the large residual on July 11, but we note it is comparable to the large north-south advection. For flight 24 on August 15 this late-afternoon flight spans the surface temperature maximum (see Figure 6 later), and we have rejected the advection terms. For flight 40 on October 13 the ABL is growing very rapidly after sunrise and the linearized budget is questionable (see section 5.5).

TABLE 5. Latent Heat Budgets

Date, 1987	Flight	$\partial q/\partial t$, W m^{-3}	$u\partial q/\partial x$, W m^{-3}	$v\partial q/\partial y$, W m^{-3}	$\partial F_\theta/\partial z$, W m^{-3}	Residual, W m^{-3}	Normalized (adv)	Residual (zero)
July 11	11	0.286 ± 0.015	0.179 ± 0.098	−0.129 ± 0.076	0.192 ± 0.117	0.144 ± 0.171	0.84	(0.55)
Aug. 15	23	0.692 ± 0.004	0.100 ± 0.024	−0.686 ± 0.161	0.282 ± 0.126	−0.176 ± 0.206	−0.85	(1.99)
Aug. 15	24	0.327 ± 0.044	−0.16 ± 0.029	−0.261 ± 0.203	0.101 ± 0.153	−0.050 ± 0.260	(−0.19)	0.87
Oct. 7	34	−0.061 ± 0.005	0.001 ± 0.25	−0.118 ± 0.012	−0.061 ± 0.093	−0.117 ± 0.098	(−1.20)	−0.00
Oct. 7	35	−0.050 ± 0.007	0.012 ± 0.024	−0.027 ± 0.013	−0.080 ± 0.051	0.015 ± 0.058	(0.26)	0.52
Oct. 11	37	0.061 ± 0.008	−0.009 ± 0.014	−0.000 ± 0.002	0.055 ± 0.009	−0.003 ± 0.018	−0.17	(0.35)
Oct. 12	39	−0.405 ± 0.029	−0.015 ± 0.033	0.033 ± 0.007	−0.332 ± 0.204	−0.055 ± 0.209	−0.26	(−0.35)
Oct. 13	40	0.114 ± 0.006	0.066 ± 0.052	−0.014 ± 0.021	0.077 ± 0.069	0.088 ± 0.89	0.98	(0.41)

Column 3–7 are all converted to units of watts per cubic meter (W m^{-3}).

These budgets indicate the observational challenge presented by the daytime evolution of the ABL. The entrainment of warm dry air into the ABL appears to be larger than expected; it increases the rise of ABL temperature and reduces the rise of moisture associated with the surface fluxes, but the uncertainties are large. *Betts* [this issue] and this paper (briefly in section 6) discuss the consequences of large ABL top entrainment for different seasons.

4.3. *Comparison of Aircraft Fluxes With Extrapolated Surface Fluxes*

The aircraft measured the sensible heat and latent heat fluxes at altitudes ranging from 70 to 100 m. On the basis of measured surface fluxes and the flux gradients with height computed from Table 2, we can estimate (independently) the fluxes, $F_{B\theta}$, F_{Bq}, at the aircraft altitude.

$$F_{B\theta} = F_{s\theta} + Z_A \partial F_\theta / \partial Z \tag{6a}$$

$$F_{Bq} = F_{sq} + Z_A \partial F_q / \partial Z \tag{6b}$$

where Z_A is the flight altitude and $\partial F/\partial Z$ is the flux gradient with height from the budget. *Betts et al.* [1990] found that the measured aircraft fluxes were underestimated. As mentioned in section 1, some of the surface flux data have been corrected following recalibration of the net radiometers used by the Bowen ratio sites. Three sources for the residual aircraft underestimate have subsequently been identified. The first, which we correct for in this paper, involved the wind gust processing. *MacPherson* [1990] found that using vertical gust velocities derived solely from the Litton inertial navigation system, rather than an algorithm which used the aircraft Doppler radar to provide the low-frequency component, increased the heat and moisture fluxes by a factor of 1.13 ± 0.02, improved the correlation coefficient, and also gave better agreement in an intercomparison with the University of Wyoming King Air aircraft. For the October flights in 1987, sufficient data were recorded to reprocess the fluxes using these so-called "Litton winds," so we used those aircraft fluxes here. Since flights in FIFE 1989 showed very similar differences between the two methods of flux processing, we felt justified in multiplying the aircraft fluxes for the July and August flights by this same factor of 1.13, to give a consistent set of aircraft flux data. Correspondingly, we have also revised the figures from *Betts et al.* [1990] by substituting recomputed fluxes where available or by multiplying by the same factor of 1.13.

Table 6 gives the ratio of the filtered aircraft fluxes, $F_{A\theta}$, F_{Aq}, to those "budget values" calculated using (6) at the flight level of the aircraft (70–100 m). The last four lines in Table 6 are the comparable revised figures from *Betts et al.* [1990], based on extrapolating the aircraft flux gradients to the surface. It can be seen that these earlier values are consistent with the grid flights, so we included them in getting a best estimate of the residual flux underestimate by the aircraft. We have divided the data in Table 6 into two groups: summer and fall. For the five summer flights in July and August the mean ratios are

$$F_{A\theta}/F_{B\theta} = 0.75 \pm 0.08 \qquad F_{Aq}/F_{Bq} = 0.84 \pm 0.06 \tag{7a}$$

corresponding to mean values of $F_{B\theta}$ = 83 W m^{-2} and F_{Bq} = 337 W m^{-2}. The mean ratios for the seven fall flights in October are

TABLE 6. Ratio of Aircraft Fluxes to Surface Fluxes Extrapolated to the Same Level

Date, 1987	Flight	$F_{A\theta}/F_{B\theta}$	F_{Aq}/F_{Bq}	Z_A,m	β_s
July 11	11	0.73	0.74	104	0.32
Aug. 15	23	0.75	0.82	100	0.34
Aug. 15	24	0.89	0.86	86	0.23
Oct. 7	34	0.80	1.21	81	4.51
Oct. 7	35	0.68	1.05	75	3.42
Oct. 11	37	0.70	1.40	72	5.68
Oct. 12	39	0.66	1.22	70	4.78
Oct. 13	40	0.64	1.45	74	3.39
	Revised Fluxes From Betts et al. [1990]				
Aug. 20	29	0.69	0.86		0.32
Aug. 20	30	0.69	0.91		0.14
Oct. 8	36	0.74	1.03		3.7
Oct. 13	41	0.75	1.26		3.6

$$F_{A\theta}/F_{B\theta} = 0.71 \pm 0.06 \qquad F_{Aq}/F_{Bq} = 1.23 \pm 0.16 \tag{7b}$$

corresponding to mean values of $F_{B\theta}$ = 221 W m^{-2} and F_{Bq} = 63 W m^{-2}. The ratios for sensible heat are less than for latent heat, and the gap widens from the summer to the fall, when the evaporation is very small. In October the aircraft latent heat flux is higher than the surface-based estimate. We have no reason to suspect that the aircraft will have different biases with season, so we suspect the surface flux data have some biases. The Bowen ratio stations (which are the majority of the surfaces flux stations) are less accurate in October, when the surface evaporation is small (E. Smith, personal communication, 1991). If we suppose that the aircraft fluxes are a fixed underestimate (R_θ, R_q, for heat and moisture, respectively), while the surface latent (sensible) heat fluxes are biased low (high) by Δ_1, Δ_2 W m^{-2}, in summer and fall, respectively, then we can reformulate (7*a*) and (7*b*) using the mean fluxes for each season, as

$$62/A_\theta = 83 - \Delta_1 \qquad 282/A_q = 337 + \Delta_1 \tag{8a}$$

$$158/A_\theta = 221 - \Delta_2 \qquad 77/A_q = 63 + \Delta_2 \tag{8b}$$

For $\Delta_1 = \Delta_2 = 0$, we retrieve the mean ratios in (7). The four equations in (8*a*) and (8*b*) give

$$R_\theta = 0.83 \qquad R_q = 0.82$$

$$\Delta_1 = 9 \text{ W m}^{-2} \qquad \Delta_2 = 31 \text{ W m}^{-2}$$

for summer and fall, respectively. This simple analysis shows that we can interpret (7*a*) and (7*b*) as being consistent with a fixed aircraft flux underestimate of about 18% (the same for heat and moisture), provided there is a bias in the measured surface Bowen ratio, which increases from summer to fall. The sense of this bias is that the mean surface latent heat flux is too low and that the sensible heat flux too high by 9 W m^{-2} in the summer and by 30 W m^{-2} in the fall. The aircraft CO_2 fluxes also generally exceeded the surface measurements in October 1987 (R. L. Desjardins, personal communication, 1990), which lends support to the conclusion that the surface latent heat fluxes were underestimated in the fall.

Our conclusion, which is tentative because of the uncertainties in the surface flux measurements, is that the residual

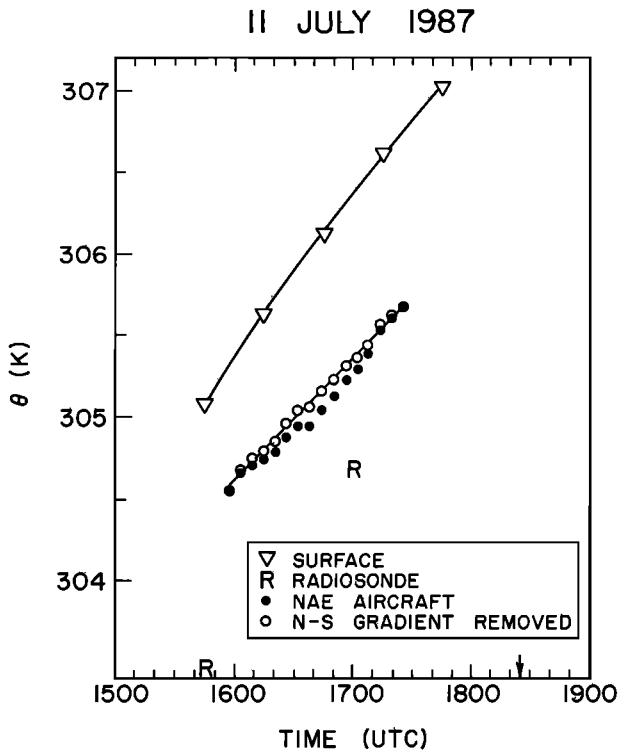

Fig. 4. Potential temperature, θ, against time for July 11, 1987, for surface, aircraft, and radiosondes. The arrow marks local solar noon.

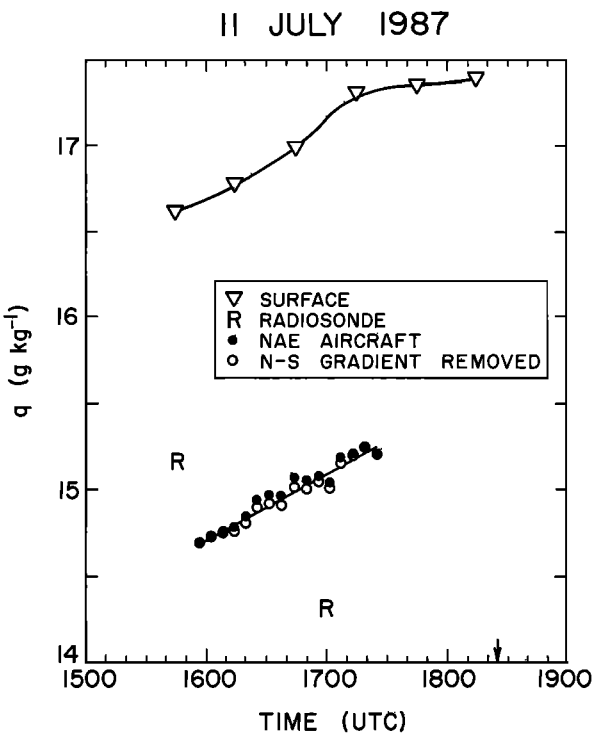

Fig. 5. As Figure 4 for mixing ratio, q.

underestimate in the aircraft flux measurements is 18 ±8%. This is entirely consistent with the loss of flux caused by filtering and undersampling of long wavelengths. The high-pass filtering of the data at 0.012 Hz (corresponding to a wavelength of 4.6 km at the usual aircraft flight speed) consistently reduced the mean flux by 17% [*Desjardins et al.*, this issue] at low altitudes. Large 75 km "regional" runs suggest that the 15-km legs flown in FIFE inadequately sample long wavelength contributions to the fluxes and that this leads to a further flux underestimate of about 4% [*Desjardins et al.*, this issue].

5. Discussion of Individual Days

We now present a more detailed discussion of the individual flight days and any analysis problems unique to them.

5.1. *July 11, 1987*

On this day of strong southerly wind (Table 1) the surface Bowen ratio was small (0.26), and β_t was small and negative at the inversion (−0.34). The mean inversion depth is not well defined by the two available soundings (Figure 2). The first sounding, at 1545 UTC, has a sharp inversion with a base near 680 m, but the second sounding has a mixed layer to 640 m capped by a deep moderately stable layer from 640 to 980 m, suggestive of a transitional structure only partly coupled to the mixed layer (Figure 3). As mentioned earlier, our inability to define mixed layer depth accurately from soundings is a weakness of our analysis. The heat budget shows a residual heating (Table 4), much larger than the error estimate, although the moisture budget is quite good.

Figure 4 shows the time trend of potential temperature θ, for an average of the surface stations (inverted triangles), a vertical average of the two radiosondes within the ABL (plotted as a symbol R at the sonde launch time), and the mean for the 16 aircraft legs (solid circles). These aircraft leg averages are the input to the linear (y, t) regression to find the north-south and time derivatives. The open circles are the leg averages with this north-south (y) gradient removed, and the thin solid curve is the linear regression fit in time to the open circles. Several things are apparent. The trend of θ at the surface appears roughly linear, but the superadiabatic layer is strengthening with time during the aircraft flight. The two radiosondes, being approximately 3-min vertical averages with different sensors, cannot be used to compute a reliable time gradient. The aircraft legs near 1645 UTC are in the south and are colder than the linear fit in time; with a south wind this corresponds to the cold advection in Table 4. Figure 5 shows the corresponding graph for the trend of mixing ratio q with time. The two radiosonde averages do not fit the trend at all. The north-south advection is smaller and the gradient somewhat less well defined. Figures 4 and 5 (and the subsequent figures) give a visual assessment of the goodness of fit of the linear regression in y and t. Tables 4 and 5 give the root-mean-square errors of the terms calculated from the gradients found by the linear regression. Where the advection is so small that the solid and open circles would overlap even in the south, we omit the open circles from the figures. An arrow indicates the time of local solar noon in Figure 4 and all subsequent figures.

The moisture budget residual is comparable to the error estimate, because the errors are quite large in both moisture advection terms and in the vertical flux divergence. Moisture budget errors are generally larger than those in the heat budget, both because the gradients are less well defined and because the errors in the inversion level moisture flux are larger than for the corresponding heat flux (see Table 2).

With A_R = 0.38, however, the heat budget shows a

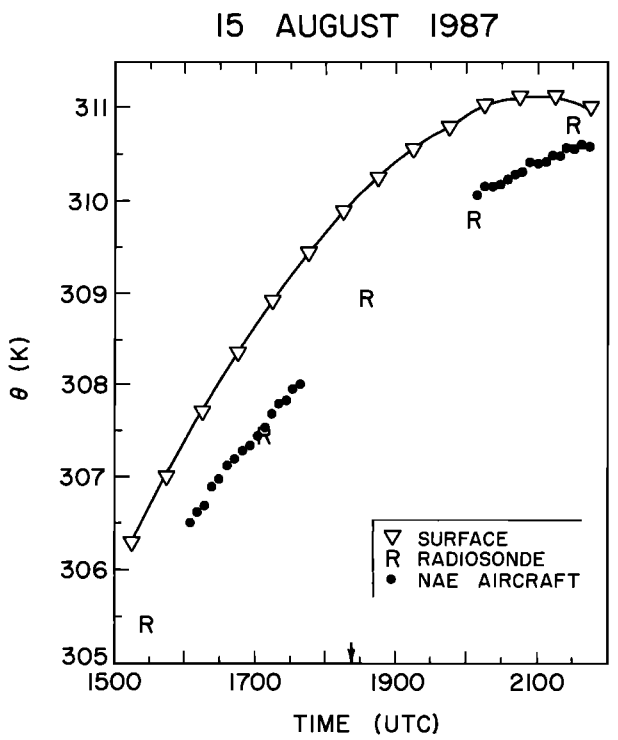

Fig. 6. As Figure 4 for August 15, 1987.

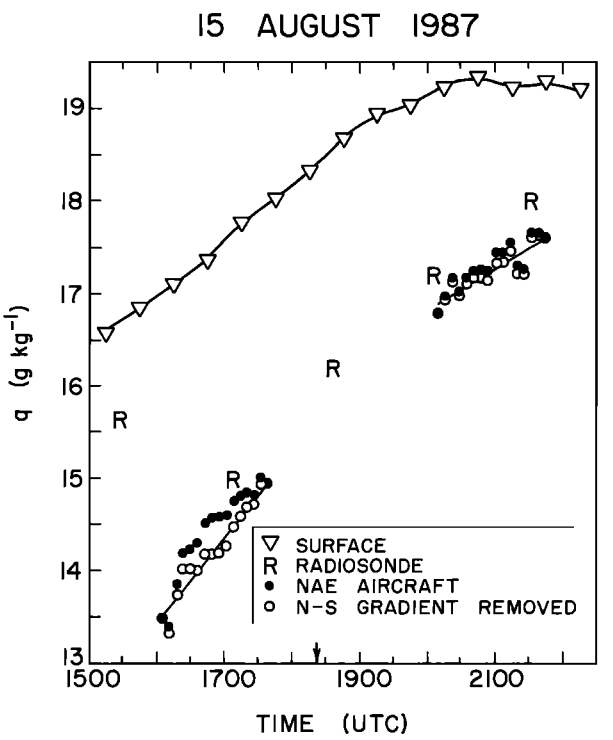

Fig. 7. As Figure 5 for August 15, 1987.

residual much larger than the error estimate, roughly equal in magnitude to the contribution of the apparent cold advection from the south visible in Figure 4. Of all the residuals from the eight flights this one is the most puzzling. Balancing the heat budget requires either more surface heat flux, more entrainment, or less cold advection, and we have no strong evidence to suggest any of these.

5.2. *August 15, 1987*

On this day of strong southerly winds there were two grid flights: one in the late morning and one in the afternoon. Again, the Bowen ratio at the surface is small, and at the inversion it is small and negative. There are five soundings and the inversion level Bowen ratio is generally falling during the day. The inversion height (not shown) increases between the soundings at 1526 and 1705 UTC, drops discontinuously between this time and the next sounding at 1834 UTC, and then increases again. Figure 6 shows much of the diurnal cycle of θ at the surface and for the ABL. The radiosonde averages track the aircraft data well on this day. During the first flight the superadiabatic layer is strengthening, but during the second it is rapidly weakening as the surface starts to cool. The aircraft data for the north-south θ advection are omitted for clarity because this gradient is so small. The morning heat and moisture budgets are satisfactory, but the afternoon heat budget has a large residual. We show the budget with and without the advection terms. The gradients in y and t appear well defined, and no reasonable change in the inversion height or inversion level fluxes will account for this large residual. The critical assumption of linear gradients in θ used by our analysis technique is suspect. The curvature of the $\theta(t)$ profile at the surface is large, since the flight is centered on the surface temperature maximum. Perhaps without advection the $\theta(t)$ sequence for the second flight would have a different curvature. Our linear regression analysis can convert a curvature in time to a linear gradient in y and hence to warm advection from the south. Using the north-south gradient found by linear regression, our budget in Table 4 shows a small warm advection (a negative term) and a larger negative residual. Without this advection the θ budget is improved. It is quite possible therefore that with sufficient curvature in $\theta(t)$ there could even be some cold advection from the south, sufficient to balance the budget. However, with one aircraft we cannot determine the N-S gradient other than by making the linear assumption. The afternoon flight on August 15 suggests that this assumption may fail as the surface starts to cool (see also the discussion of October 7 in section 5.3).

Figure 7 shows the corresponding q plot. Four of the five soundings follow the aircraft trends well. The surface to 100 m (aircraft) gradient in q is largest in the morning and starts to fall further during the second flight as the surface rise of q stops. There is moist advection from the south during the day that plays an important role in the q budget, although the errors in this q gradient and the moisture budget are larger than in the sensible heat budget. The inversion level moisture flux increases during the day (Table 2) as the inversion level Bowen ratio becomes less negative, so $\partial q/\partial t$ falls as the moistening of the layer, both by vertical flux divergence and moist advection, drops. Note that for the second flight, near 2100 UTC, two legs are significantly drier, coincident in time with a small drop in the surface q mean (a 30-min average), suggesting a brief period of advection of drier air over the FIFE site during this time. The time sequence of q at the surface also shows a maximum near the surface temperature maximum; the q budget with zero advection has a larger residual for $A_R = 0.38$, but both normalized residuals are ≤ 1.

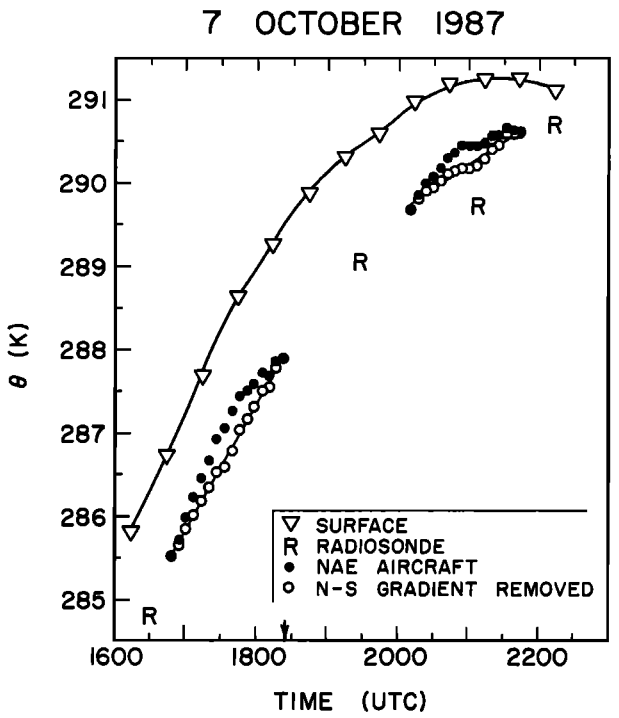

Fig. 8. As Figure 4 for October 7, 1987.

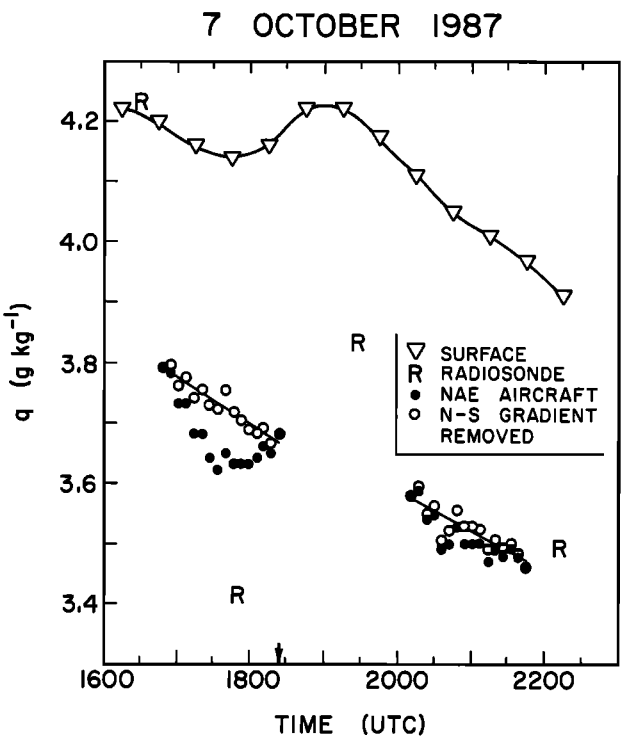

Fig. 9. As Figure 5 for October 7, 1987.

5.3. *October 7, 1987*

There were again two grid flights on October 7, which had weaker winds from the north. In October the surface vegetation has largely died, the surface Bowen ratio is large, and q values are small. The soundings show important changes at the inversion, which are seen down to the surface, especially in $\partial q/\partial t$ (see Figure 9). For the morning flight the inversion height is around 780 m, with an inversion Bowen ratio initially around -0.8. However, the sounding at 1747 UTC (not shown) toward the end of the aircraft pattern shows that a dry q layer above has disappeared, and there is no drop of q at the weak inversion. Simultaneously, the surface data shows a change from drying to moistening, presumably related to the cessation in the entrainment of drier air at the inversion. Shortly afterward (1830–1900 UTC) the ABL breaks through into a deep, nearly adiabatic layer above, with $\theta \approx 288.5$ K, and rapidly deepens to a depth $Z_i \approx 1575$ m. Its top remains at that depth, where there is a stable stratification, for the rest of the day. The inversion Bowen ratio returns to approximately -0.5, and the drying of the ABL resumes because the inversion level q flux exceeds the small evaporation at the surface (Table 2). These changes have a large impact on our budget analysis. Figure 8 shows the time trend of θ. At first sight there appears to be cold advection for both flights (winds are from the north; see Table 1). Both the morning and the afternoon θ budgets (Table 4) have positive residuals, larger than the error estimate, which are comparable to the northerly "cold advection." In the afternoon the surface $\partial\theta/\partial t$ shows marked curvature as the superadiabatic layer cools and the surface heat flux falls (while the inversion height and Bowen ratio change little), so it is again possible (as on August 15) that some of the curvature in the aircraft profile is a real-time dependence and is not caused by the y gradient. For flight 34, in the morning, there is a distinct change of slope in $\partial\theta/\partial t$ in the aircraft data and at the surface around 1730 UTC, as the mixed layer breaks through a weak inversion and rapidly deepens. This change is very clear in Figure 9 which shows the q trends with time. For the morning flight the negative residual in the q budget is comparable to the y advection derived from the linear regression. However, when we inspect Figure 9, we see similar time changes at the surface and aircraft level (80 m), which strongly suggests that our linear assumption is here also in error. The aircraft trend faithfully reflects the q minimum seen at the surface and is almost certainly associated with the change in q flux at the inversion, which we discussed earlier. Thus the aircraft leg means most likely reflect a real-time trend. Since the q minimum occurs close to the time of the southern legs of the grid pattern, however, the linear regression incorrectly interprets it as a y gradient of q. The limitation of our linear regression analysis using single aircraft data is again apparent. Fortunately, there is sufficient coincident surface and sounding data to give a qualitative interpretation of the residual error, as well as some physical appreciation of how inversion level processes are coupled right down to the surface.

5.4. *October 11, 1987*

The grid flight on October 11 (with a very light southwesterly wind) also spanned a major change in inversion level q and in the corresponding inversion level q flux. During the aircraft pattern the ABL depth was in the range of 900–1100 m, but the soundings give very different inversion level Bowen ratios. Prior to the grid flight, two soundings have a thin dry layer in the range 900–1000 m, just above the ABL, and a corresponding inversion Bowen ratio of approximately -0.7. Early in the aircraft pattern the ABL top reached this level, and the dry layer disappeared. Subsequently, there

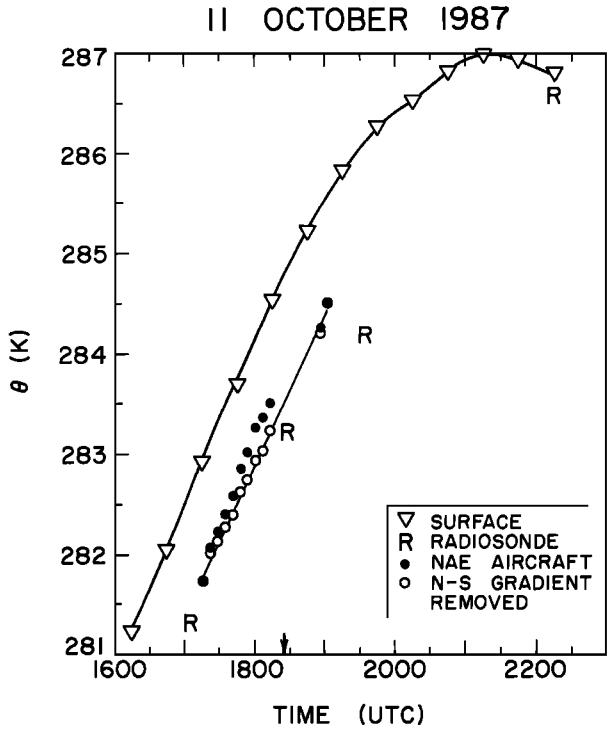

Fig. 10. As Figure 4 for October 11, 1987.

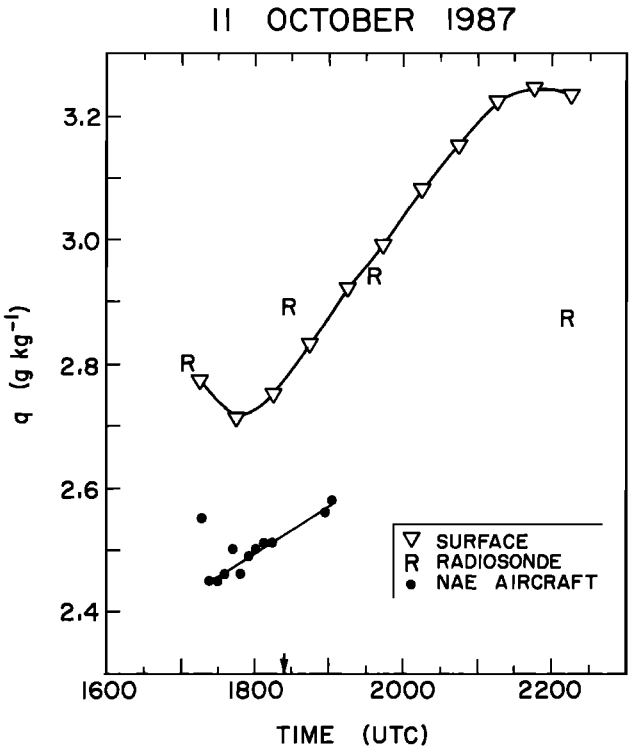

Fig. 11. As Figure 5 for October 11, 1987.

was no drop of q at the ABL top, and so no q flux associated with entrainment. Figure 11 suggests this change occurred quite suddenly near 1725 UTC, shortly after the start of the aircraft flight. We therefore excluded the first two aircraft legs from the budget analysis. The advection terms are small on this day, because the winds are very light. Figure 10 shows the time change of θ. The budget residual is within the error and represents a close balance of heating and vertical flux divergence. Figure 11 shows the time change of q. The surface q shows a minimum at 1745 UTC (a 30-min average from 1730 to 1800), while the aircraft data shows a sharp fall between the first and subsequent legs. The linear regression used only the data from legs 3 to 18 (legs 11–16 are also missing because of bad data). We believe that this increase of q with time corresponds to the very large Bowen ratio (small q flux) at the inversion seen in the 1826 UTC and subsequent soundings. The q budget is satisfactory.

5.5. *October 12, 1987*

October 12 had very light winds from the WNW, and the ABL was uniformly warming and drying throughout the aircraft grid flight. The ABL was shallow and growing slowly, with a depth near 500 m; the surface Bowen ratio was large, and at the inversion $\beta_i \approx -0.5$ and fairly steady. The inversion level q flux is thus larger than at the surface (Table 2), so that the ABL dries.

The aircraft flew a double coarse grid pattern this day, consisting of four legs from north to south at double the y spacing shown in Figure 1, repeated a total of 4 times. We assume linearity of the y and t gradients to perform the regression analysis, but now we can see a repeated pattern. Figure 12 shows the (θ,t) plot. It is warmer to the south on both patterns, so with a weak northerly wind component there is clearly weak cold advection. The advection terms are small (Table 4) compared to the errors in the vertical flux gradient. These errors are large because the ABL is shallow and there is uncertainty both as to its depth and as to the value of A_R, the entrainment parameter. The residual is smaller than our error estimate. Figure 13 shows the q

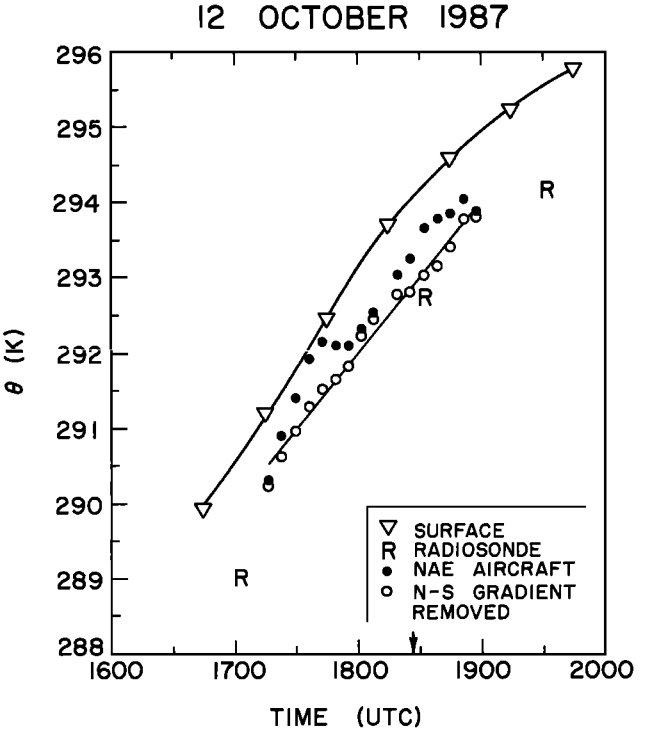

Fig. 12. As Figure 4 for October 12, 1987.

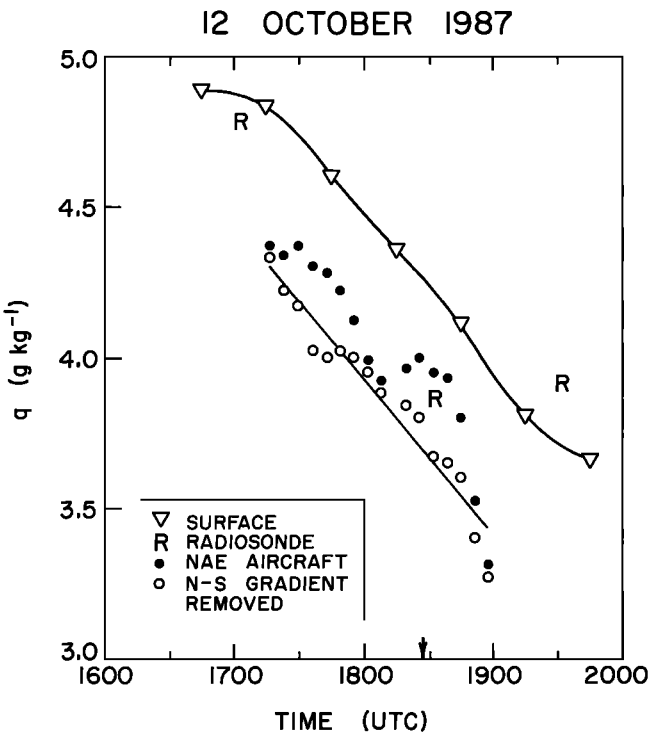

Fig. 13. As Figure 5 for October 12, 1987.

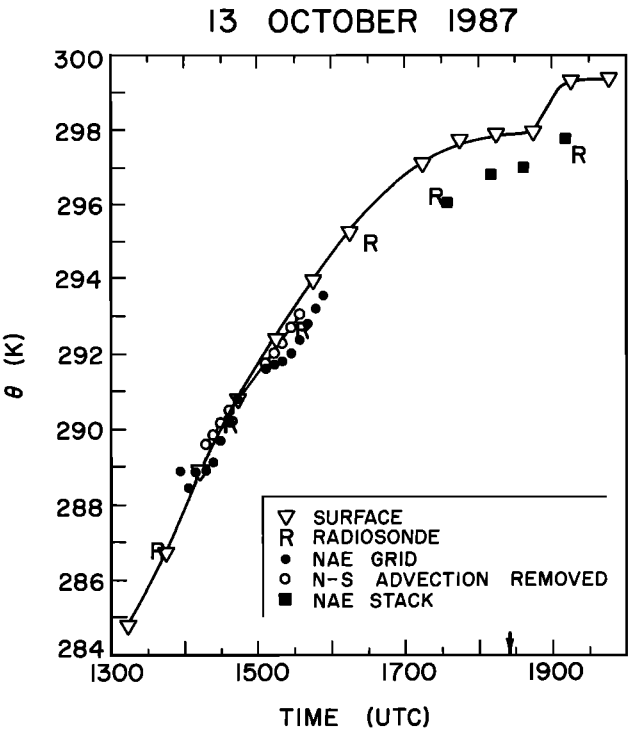

Fig. 14. As Figure 4 for October 13, 1987.

change with time, again showing a repeated y gradient pattern. Again, however, the advection terms are small compared with $\partial q/\partial t$ and $\partial F_q/\partial Z$. The q budget balances well within the errors. The primary reason for the strong drying of the layer is entrainment of dry air at the inversion. Uncomplicated budgets such as these give us confidence in our mean value of A_R.

5.6. *October 13, 1987*

This day required the most subjective analysis because of its complexity. We would have excluded it, except that it shows fascinating structure and was the only grid flight documenting the initial growth of the mixed layer in the early morning. In addition, another flight later in the day was analyzed by *Betts et al.* [1990]. The ABL depth grew from about 100 m to about 350 m during this early morning aircraft flight. The wind was strong, from the SSW. The first three legs were in the entrainment layer of negative heat flux, and these were excluded from the analysis. The aircraft again flew a repeated coarse grid pattern, as on October 12. The inversion level Bowen ratio dropped sharply between the soundings at 1437 and 1535 UTC, and the q data suggest the change happened sharply at 1530. The last three aircraft legs show a sharp fall of q, mirroring that seen in the surface data. Therefore we also excluded these three legs also from the regression analysis.

Figure 14 shows the θ trends for the day. The pattern was again a double minigrid, showing large cold advection with a strong southerly wind. The first flight started in the early morning when the mixed layer was barely 100 m deep, so both θ and ABL depth are changing very rapidly. The θ budget shows a normalized residual of ≥ 1, and it is possible that the cold advection, derived from only 10 legs, has been overestimated. The four solid squares (labeled NAE stack) represent four stack averages for the afternoon flight, one of those analyzed by *Betts et al.* [1990]. There was still cold advection for this flight, although the magnitude was smaller.

Figure 15 shows the corresponding q trends. The remarkable feature, mentioned earlier, is the change from moistening to drying that occurs near 1530 UTC, apparently associated with a sharp fall in the inversion level Bowen ratio from

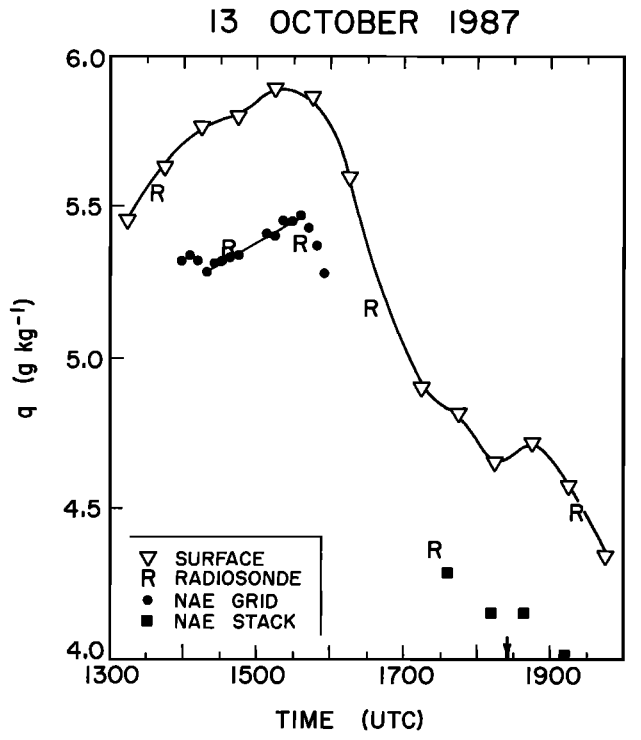

Fig. 15. As Figure 5 for October 13, 1987.

about −2 to values as small as approximately −0.3 later in the day. Our linear fit to the q data (solid curve), which excludes both the first three legs (which are in the entraining layer) and the last three legs (after q falls abruptly), shows no significant q advection. We see once again in Figure 15 the dramatic coupling between changes in inversion level entrainment and the time changes in the ABL all the way down to the surface.

6. Discussion and Conclusions

This paper extends the budget analysis begun by *Betts et al.* [1990] to the FIFE 1987 grid pattern flights by the Canadian NAE Twin Otter research aircraft. Several preliminary conclusions by Betts et al. are confirmed by this different data set. The aircraft consistently underestimate the sensible and latent heat fluxes compared with the surface data, corrected using vertical gradients to the same level. However, by making two corrections to the data, it has been possible to reduce these underestimates considerably from those shown by *Betts et al.* [1990]. The mean surface flux measurements have been reduced following a recalibration of the net radiometers used by the Bowen ratio surface flux sites. In addition, the aircraft fluxes have been increased by 13% as a result of using vertical eddy winds based solely on the Litton inertial navigation system. There remains a residual flux underestimate by the aircraft relative to a mean of the surface flux sites, which we estimate to be about 18 ± 8%. This is of the order expected [*MacPherson*, 1990] from the high-pass filtering at 0.012 Hz and the undersampling of long wavelength contributions (the FIFE runs were only 15 km long). We suspect that there may also be biases in the heat and moisture fluxes from the surface sites, because the ratio of aircraft to surface fluxes is lower for sensible than for latent heat. The gap is small in July and August but much larger in October. In October, when the surface latent heat fluxes are very low (≈60 W m^{-2}) after most of the grassland vegetation has died, the aircraft fluxes are in fact larger than the surface mean by 23 ± 16%, roughly 15 W m^{-2}. Since we have no reason to expect the aircraft system to behave differently with season, this would suggest that the surface sites may be undersampling the area mean evapotranspiration by as much as 30 W m^{-2} in October. This value seems large. It is possible that the vegetation in the gullies is still transpiring in October and that this contributes to the flux seen by the aircraft but is not well sampled by the surface stations. A more likely reason is a larger systematic bias in the Bowen ratio stations in October, when the surface Bowen ratio is large (E. Smith, personal communication, 1991). We show that the October aircraft to surface flux ratios are consistent with an 18% aircraft flux underestimate and a surface flux bias of 31 W m^{-2}, with the surface latent (sensible) heat flux being low (high) by this amount.

A second, somewhat surprising result of great importance to FIFE and ABL research in general is that the inversion level fluxes caused by ABL top entrainment appear to be about double those used in many simple mixed layer closure models. *Betts et al.* [1990] estimated a mixed layer closure parameter $A_R = 0.43 \pm 0.12$, and here we found 0.38 ± 0.16. The long-accepted value for free convective boundary layers has been $A_R \approx 0.2$. Although some flight days had strong winds, when turbulence generated by surface shear might be expected to drive additional entrainment, others with high entrainment had light winds. The impact of this greater entrainment is threefold: the ABL grows more rapidly, warms more rapidly, and entrains dry air more rapidly. This has a big impact on the ABL moisture budget. When the surface moisture flux is large as in the summer, it reduces the moistening of the ABL; when the surface moisture flux is low, as in the fall, it produces a drying of the ABL during the day. These solutions for idealized mixed layers are discussed by *Betts* [this issue]. This possibility of high-entrainment rates is so important that it needs further study. The lidar studies of mean ABL growth might be used to estimate mean entrainment rates. Future experiments should include continuous profiling of boundary layer depth and inversion strength by surface-based systems.

The budget analyses using a mixed layer model were generally encouraging, although the errors, particularly in measuring horizontal advection, are significant. Both *Betts et al.* [1990] and this study found that a single aircraft could estimate the horizontal advection on the 15-km scale of the FIFE network, provided the gradients in time and space remained approximately constant during a flight. The error in measuring the north-south advection in high winds is, however, quite large, with north-south pattern sizes of only 10–15 km. In two afternoon flights, which spanned the surface temperature maximum, the nonlinearity of $\partial\theta/\partial t$ introduced significant but unknown errors into the estimate of the north-south advection. We recommend that flights be made nearer local noon when the rise of temperature is more linear. The repeated minigrid pattern has a clear advantage in separating the time and space derivatives using a single aircraft, because the pattern associated with advection is repeated.

This analysis has shown the importance of the FIFE network of integrated observations. The sonde data give the crucial inversion depth and the estimate of the inversion level Bowen ratio. Sudden changes in entrainment at the inversion can be seen reflected in both the aircraft and the surface data. The comparison of the aircraft and surface time trends showed us cases where the aircraft pattern included sudden transitions, and the gradients did not satisfy the linearity conditions in time. We can now use simple mixed layer models for the growth of the cloud-free ABL over the FIFE network with some confidence and some awareness of the variability associated with horizontal advection and changes in the thermodynamic properties of the air entrained at the inversion.

Acknowledgments. A. K. Betts was supported by NASA-GSFC under contract NAS5-30524 and NSF under grant ATM90-01960. R. L. Desjardins and J. I. MacPherson gratefully acknowledge funding from NASA, the National Research Council, and Agriculture Canada for their participation in FIFE 1987. The assistance of the staff of National Aeronautical Establishment in collecting the data is also acknowledged. We thank the reviewers for their helpful comments.

References

Betts, A. K., Non-precipitating cumulus convection and its parameterization, *Q. J. R. Meteorol. Soc.*, *99*, 178–196, 1973.

Betts, A. K., Mixing line analysis of clouds and cloudy boundary layers, *J. Atmos. Sci.*, *42*, 2751–2763, 1985.

Betts, A. K., Budget analyses of the FIFE atmospheric boundary layer budget methods, *J. Geophys. Res.*, this issue.

Betts, A. K., R. L. Desjardins, J. I. MacPherson, and R. D. Kelly, Boundary layer heat and moisture budgets from FIFE, *Boundary Layer Meteorol., 50*, 109–137, 1990.

Brutsaert, W., and M. Sugita, The extent of the unstable Monin-Obukhov layer for temperature and humidity above complex hilly grassland, *Boundary Layer Meteorol., 51*, 383–400, 1990.

Carson, D. J., The development of a dry inversion-capped convectively unstable boundary layer, *Q. J. R. Meteorol. Soc., 99*, 450–467, 1973.

Desjardins, R. L., J. I. MacPherson, P. Alvo, and P. H. Schuepp, Measurements of turbulent heat and CO_2 exchange over forests from aircraft, in *The Forest-Atmosphere Interaction* edited by B. A. Hutchison and B. B. Hicks, pp. 645–658, D. Reidel, Norwell, Mass., 1986.

Desjardins, R. L., J. I. MacPherson, P. H. Schuepp, and F. Karanja, An evaluation of airborne eddy flux measurements of CO_2, water vapor and sensible heat, *Boundary Layer Meteorol., 47*, 55–69, 1989.

Desjardins, R. L., P. H. Schuepp, J. I. MacPherson, and D. J. Buckley, Spatial and temporal variations of the fluxes of carbon dioxide and sensible and latent heat over the FIFE site, *J. Geophys. Res.*, this issue.

MacPherson, J. I., Wind and flux calibrations on the NAE Twin Otter, *NAE Lab. Tech. Rep., LTR-FR-109*, Inst. for Aerosp. Res., Ottawa, Ont., Canada, Feb. 1990.

MacPherson, J. I., R. L. Desjardins, E. Brach, P. Alvo, and P. H. Schuepp, Preliminary evaluation of aircraft-mounted sensors for gaseous exchange measurements, in *Proceedings of the 17th Conference on Agriculture and Forest Meteorology*, pp. 13–17, American Meteorological Society, Boston, Mass., 1985.

Stull, R. B., The energetics of entrainment across a density interface, *J. Atmos. Sci., 33*, 1260–1267, 1976.

Stull, R. B., *An Introduction to Boundary Layer Meteorology*, 666 pp., Kluwer Academic, Boston, Mass., 1988.

Sugita, M., and W. Brutsaert, How similar are temperature and humidity profiles in the unstable boundary layer?, *J. Appl. Meteorol., 29*, 489–497, 1990.

Tennekes, H., A model for the dynamics of the inversion above a convective boundary layer, *J. Atmos. Sci., 30*, 558–567, 1973.

A. K. Betts, R.D. 2, Box 3300, Middlebury, VT 05753.

R. L. Desjardins, Land Resource Research Centre, Agriculture Canada, Ottawa, Ontario, Canada K1A 0C6.

J. I. MacPherson, Institute for Aerospace Research, Ottawa, Ontario, Canada K1A 0R6.

(Received February 7, 1991;
revised November 29, 1991;
accepted December 16, 1991.)